

TUNABLE IMBIBITION OF MOLTEN METAL ON A ROUGH SURFACE

Wen Liu and Dusan P. Sekulic*
 *Author for correspondence
 Department of Mechanical Engineering,
 University of Kentucky,
 Lexington, KY, 40506,
 USA,
 E-mail: sekulicd@engr.uky.edu

ABSTRACT

The imbibition of a molten metal system on a rough inert surface was studied in situ at an elevated temperature by using hot stage microscopy. The non-uniform spreading pattern was registered. The imbibing direction with larger observed imbibition distance was proved to be associated with the orientation of the topographical features of the substrate. The kinetics data indicate that the imbibing follows Washburn relation ($\xi \sim t^{0.5}$) during the early stage and then deviates due to the impact of finite-size source material before the ultimate asymptotic termination. A theoretical model was utilized to describe the Washburn-type imbibition during the early capillary-viscous stage, and to explain the deviation of the imbibing kinetics from $\xi \sim t^{0.5}$. This study offers (i) experimental evidences that the molten metal flow can be controlled by a topographically altered substrate, and (ii) a theoretical framework to describe and predict the molten metal flow on such a substrate.

INTRODUCTION

Wetting and capillary phenomena have been of key interest for a long time [1]. As reviewed in [2], the imbibition phenomenon is of a significant importance for fluid transport in nature, and in industrial processes such as printing, painting, oil recovery, and fabrication of composite materials. Imbibition processes have also been treated as simplified models for the absorption of water in soils, as mentioned in [3]. A controlled or tunable spreading (imbibition) process is always desired. For example, a uni-directional spreading of deionized water was achieved by introducing a topographical structure fabricated on a polymer surface [4]. An anisotropic spreading on a micro-wrinkled PDMS surface with varying roughness aspect ratio was observed and studied [5]. Chemical pattern was also previously utilized for controlling the wetting direction [6]. However, a very few studies have been devoted to the kinetics of a controlled spreading/imbibition of liquid metal on metallic surfaces at elevated temperatures.

Recently, Liu and Sekulic proposed analysis and associated models of spreading kinetics of isotropic as well as anisotropic imbibition of molten metal and organic liquid systems on various manufactured intermetallic surfaces [7-9]. In that series of studies, the imbibition process of liquid metal or organic liquids at an elevated temperature or room temperature levels was described to be associated with (i) liquid properties, i.e., surface tension and viscosity, and (ii) surface topographical details, i.e., porosity/tortuosity and permeability.

NOMENCLATURE

θ	[deg]	Contact angle
σ	[mN/m]	Surface tension
μ	[mPa·s]	Viscosity
x	[m]	Cartesian axis direction
y	[m]	Cartesian axis direction
Special characters		
α	[deg]	Groove angle
τ	[-]	Tortuosity
η	[m]	Filling factor
h_0	[m]	Average height of a micro groove
R_{di}	[-]	Directional imbibition ratio
ξ	[m]	Imbibition distance
Subscripts		
di		Directional imbibition
x		Cartesian axis direction
y		Cartesian axis direction
0		Initial

In this study, with a new set of empirical data (see Fig. 2 b and c), authors continue to explore the feasibility of a tunable imbibition process of molten metal on a manufactured surface and offer an independent validation of the previous theoretical analysis by using additional empirical data. An objective of this paper is to demonstrate that a change of topographical features of the rough surface can be used for tuning the preferential imbibition. We first introduce a detailed discussion of the experimental procedure for manufacturing the microstructured

intermetallic surfaces. The spreading tests at elevated temperatures are described next. Then a detailed analysis of imbibition phenomena and associated surface characterization are provided. At last a brief theoretical analysis and discussion brings a fundamental understanding of the proposed phenomenological observations.

MATERIALS AND EXPERIMENTAL PROCEDURES

The substrate was manufactured from a virgin copper sheet by using a method of hot dipping. A copper plate was dipped into the molten Sn at 260°C, then the re-solidified Sn coating was etched away to expose the IMC (intermetallic) layer formed at the interface, [10]. The manufacturing procedure was as follows, [10]:

(i) Etch a copper substrate of a high purity (99.9%) first in a mild acid (95% ethanol + 3% HCl + 2% H₂O) for 30 seconds.

(ii) Deposit plate with RMA (mildly activated rosin flux) flux [EC-19S-8, Tamura Corp.], and then dip into a pure molten Sn at the temperature of 260°C for 10 s, and quickly pull out.

(iii) Age the samples at 127°C for 10 days to obtain the Cu₆Sn₅/Cu₃Sn/Cu ternary layer.

(iv) Age the samples at 150°C for 10 days to obtain the Cu₆Sn₅/Cu₃Sn/Cu ternary layer.

(v) Remove the remaining Sn residue from the plate surface: suspend samples vertically and immerse in an agitated solution of 1% HCl in methanol, for approximately 20 min.

(vi) Ultrasonically clean the samples in soapy water, rinsed with water, and ultrasonically clean again in ethanol.

The steps (iv) and (v) were repeated for three times, the coupons were rinsed in methanol and ultimately dried in air. Subsequently, the so manufactured substrate was exposed to an experimental procedure aimed at establishing the kinetics of liquid metal spreading.

The substrate sample described with step (i), (ii), (v) and (vi) is designated as IMC1. The substrate sample described with steps (i), (ii), (iii), (v) and (vi) is named as IMC2. Finally, the substrate sample described with steps (i), (ii), (iv), (v) and (vi) is referred as IMC3. The Imbibition kinetics on IMC1 and IMC3 have been studied and modelled by the authors recently [7-9]. In this paper, we include previously not discussed data for IMC2.

Note that the aging process at an elevated temperature level allows a further reaction between Cu and Sn caused by the gradient of Sn concentration. Therefore the size and morphology of intermetallic grains will be altered to obtain an IMC2 or IMC3 surface, leading to an anisotropic imbibition phenomenon.

The hot stage microscopy, figure 1, was used to analyze kinetics of the triple line movement. A substrate coupon having overall dimensions of 10 mm × 10 mm × 0.3 mm is positioned within the chamber of the LINKAM THMS 600 hot stage installed on an OLIMPUS BX51M optical microscope. A solder specimen was covered with a thin layer of RMA flux [EC-19S-8, Tamura Corp.]. The chamber was filled with ultra high purity N₂ (99.999%), after purged with nitrogen for 120 minutes before an initiation of the heating/cooling cycle.

Purging has secured at least 30 chamber's volume replacements. The heating cycle consists of a ramp up, dwell and quench.

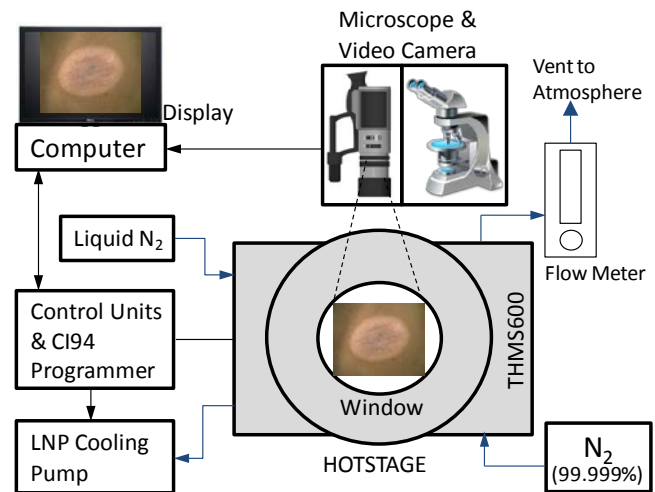


Figure 1 Configuration of the advanced hotstage microscopy equipment for imbibition tests at an elevated temperature level

The heating ramp-up was facilitated with 100°C/min and the cooling ramp-down was 80°C/min. Temperature stability was at the level of 0.1 K. Verification of the actual solder temperature was performed by comparing temperature readings for a given instant of time at the onset of melting, with the eutectic solder melting point temperature known. It is established that this temperature was recorded with a consistent bias (due to thermal contact resistance along the conductive path from the silver block heater to the solder pellet) of less than 7K at the 473 K temperature level. Correspondingly, temperature readings were corrected and the bias was eliminated. The series of thermal contact resistances includes (i) Ag heating block - quartz glass interface, (ii) quartz - glass - interface - substrate, and (iii) substrate-solder interface, in presence of flux. The peak temperature is set to be consistently 30K above the liquidus temperature of the corresponding solder. During the heating/cooling cycle, digital imaging is performed with the 22 frames/s digital camera system. Movie clips were digitally decomposed into individual frames and associated with digitally recorded corresponding substrate temperature histories. The triple line was approximated with an instantaneous equivalent perimeter locus of points (representing the solder spread perimeter), see figure 1. Measurements of the triple line locations were performed using (i) UTHSCSA® imaging tool software, and (ii) Image-Pro PLUS® software. The uncertainty in determining linear dimensions was smaller than 3%. The uncertainty was estimated by comparing measurement results of the same test conducted by two independent readings using image processing software. The dwell at the constant peak temperature during spreading lasts for 120 seconds. Solidification starts in average 100 seconds upon termination of the spreading observation period.

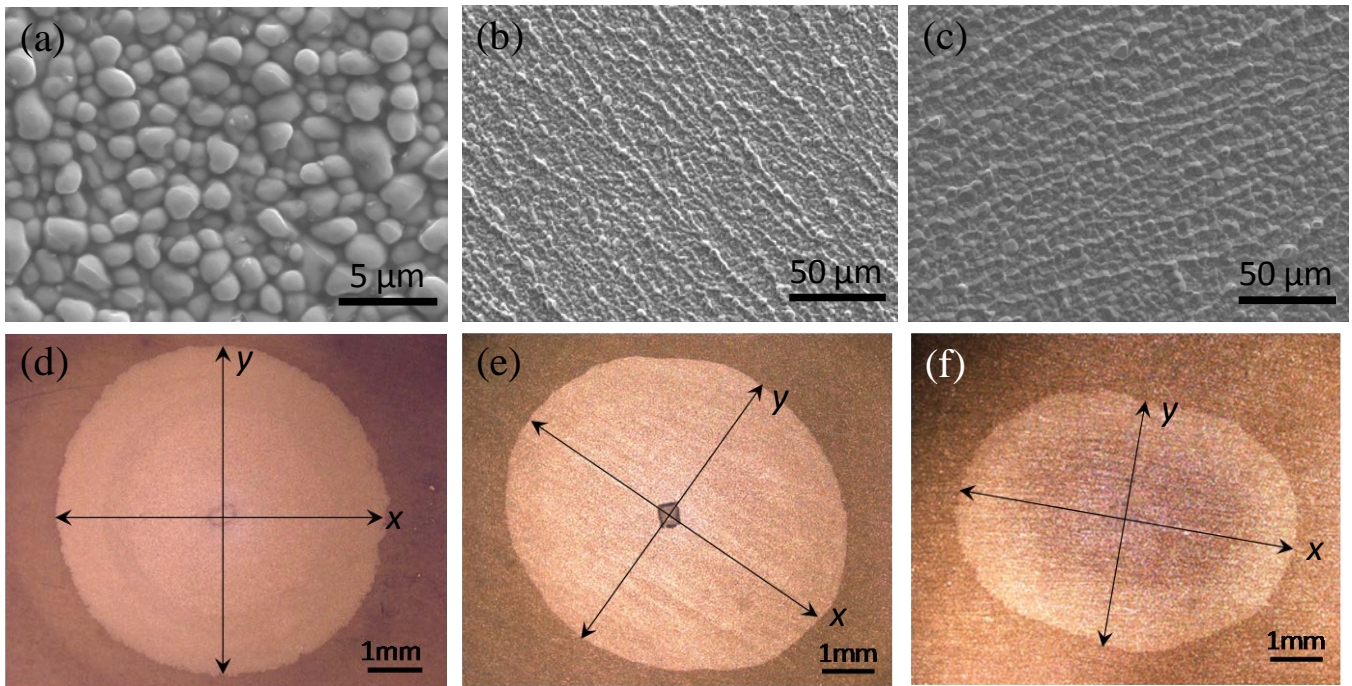


Figure 2 (a) (b) and (c) offer SEM images showing topographical features of an IMC1, IMC2 and IMC3 substrate respectively; (d) a final circle pattern resulted from imbibing of eutectic Pb-Sn solder on an IMC1 substrate; (e) an elliptical pattern generated from eutectic Pb-Sn imbibing on an IMC2 substrate; (f) an elliptical imbibition patten for eutectic Pb-Sn on an IMC3 substrate, note the ratio of the length of long axis x to the short axis y is larger than that in the case for IMC2. (Note: figure 2 (c) is taken from [9])

The solder used in this study represents an eutectic tin lead solder (Sn37Pb) with a surface tension of ~ 400 mN / m, and a viscosity of ~ 2.7 mPa·s at molten state at ~ 473 K [11]. The contact angle is estimated as 25 degree as reported in [11].

EXPERIMENTAL OBSERVATION AND RESULTS

Figure 2 offers three different sets of imbibition tests of a molten metal imbibition on IMC1, IMC2 and IMC3 surfaces, respectively. The presented frames were extracted for the purpose of this study from the movie clips generated during real time, in situ monitoring of the imbibition of the solder, [10]. It can be noticed that IMC1 has a random but uniform distribution of IMC grains. IMC2 and IMC3 feature a spatial orientation of grain structures of larger size. The difference between imbibition of the same molten metal system, i.e., eutectic Pb-Sn solder, on such three different surfaces is quite noticeable. Figure 2 (d) indicates that the final imbibition pattern of a molten solder on an IMC1 substrate is almost a perfect circle. Figure 2 (e) and (f) offer an elliptical imbibition patten for a molten solder on an IMC2 and IMC3 substrate, respectively. Note that the ratio of the orthogonal long and short axi of the imbibition pattern, which will be referred to as *directional imbibition ratio* R_{di} is different for IMC2 and IMC3. It is clear that directional imbibition ratio of an imbibition on IMC2 is smaller than that of IMC3 and this difference is consistent for at least three sets of empirical data for IMC2 and IMC3.

Figure 3 offers the quantitative analysis of directional imbibition ratios for the imbibition on IMC1, IMC2 and IMC3. The microstructured surface generated from a longer aging process is associated with a larger R_{di} .

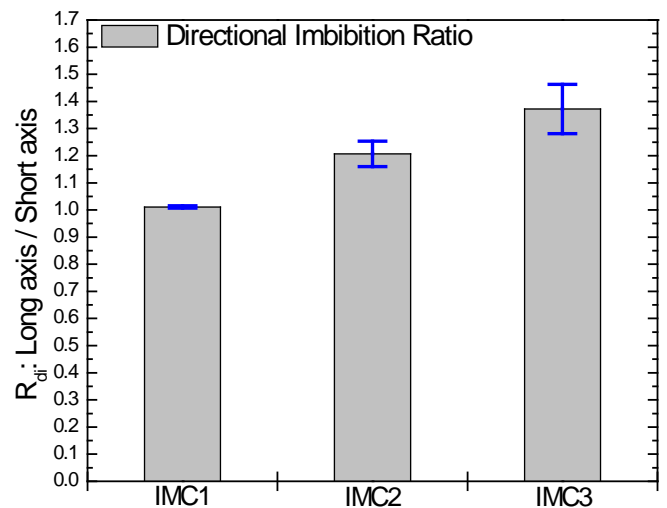


Figure 3 Ratios of the length of long axis to short axis for IMC1, IMC2 and IMC3 substrates.

The directional imbibition ratios R_{di} of cases for IMC1, IMC2 and IMC3 are 1.01 ± 0.01 , 1.21 ± 0.05 and 1.37 ± 0.09 , respectively. The average empirical data and associated

standard deviations were determined by multiple measurements for three independent imbibition tests for each IMC substrate. The measurements were performed with Image Pro software with an estimated uncertainty of ~3% for linear length determination.

It should be noticed that the imbibition processes of molten eutectic solder on IMC1 and IMC3 have been successfully studied by authors in their recent work [7-9]. This includes (i) topographical characterization and (ii) kinetics analysis and modelling. The new and independent empirical evidence for IMC2 as shown in figure 2 (b) and (e), further confirms the influence of topographical alterations on the imbibition behavior of a molten metal system. The results indicate that the imbibition could be tuned by surface manufacturing techniques.

Figure 4 (a) and (b) offer the AFM scans of surface topographical features for IMC3 and IMC2, respectively. The scanning was conducted for both cases on a random substrate area of $50 \times 50 \mu\text{m}$. It can be noticed that the micro grains on IMC2 substrate are more compact and smaller than those on IMC3. Due to an aging process at a higher temperature IMC3 substrate features more pronounced grain orientation and so formed parallel surface grooves along a certain direction. It is proved that such grain orientation is associated with the direction of the long axis of the elliptical imbibition pattern [9]. It should be noticed that the difference between the directional imbibition ratios of IMC2 and IMC3 cases arise from their topographical features because the same molten metal system was used.

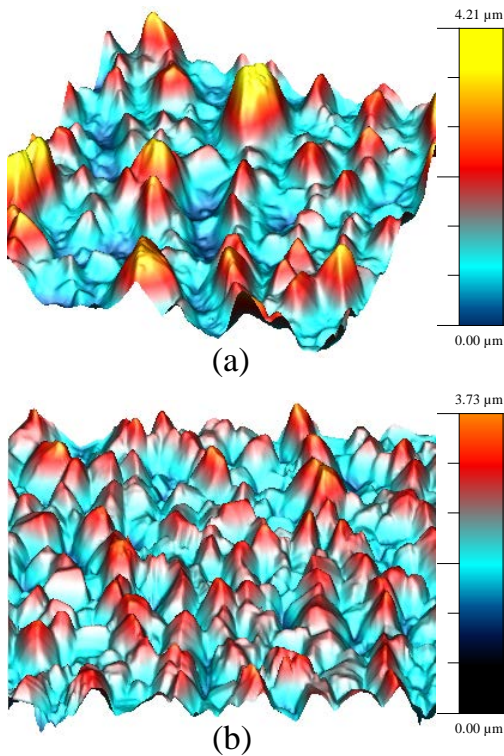


Figure 4 AFM scanning results indicate the topographical features of (a) IMC3 and (b) IMC2 substrates. (The scanning area is $50 \times 50 \mu\text{m}$)

Figure 5 offers the kinetics data of imbibition on all three types of microstructured surfaces in a log-log scale. The difference between them implies that the kinetics is influenced, hence can be tuned by the topographical features of the surface. It should be pointed out that the imbibition within capillary-viscous stage of all three cases follows the Washburn-type relation and terminate with an asymptotic ending.

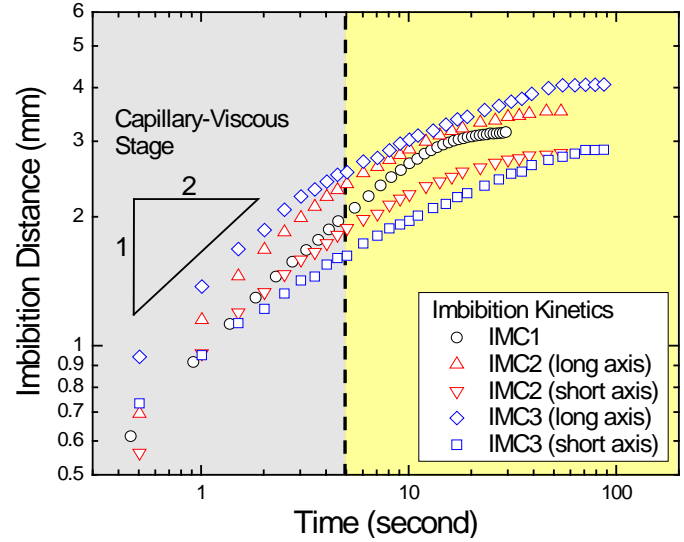


Figure 5 Kinetics of imbibition on IMC1, IMC2 and IMC3 in a log-log scale, respectively. Note that the kinetics follows Washburn relation within capillary-viscous stage. (Note the kinetics data for IMC1 and IMC3 are adopted from [7] and [9], respectively.)

THEORETICAL ANALYSIS

The theoretical model for kinetics has been established and verified for a uniform imbibition on a complex topographical substrate like IMC1, [7], as well as for preferential imbibition on an anisotropically microstructured surface as IMC3, [9]. For the sake of completeness, a brief discussion of the approach is given next. The model was built based on the Darcy's law and mass conservation principle. Following [9], we consider the rough substrate as a two dimensional porous medium, hence by introducing the tortuosity. Mass conservation has been applied to the differential domain at the imbibition front. The flow rate is described in an agreement with the Poiseuille's law. The kinetics of a preferential imbibition on IMC2 during capillary-viscous stage could be described as

$$\xi^2 = \frac{\eta_{0,\xi} h_0 \sigma}{4\pi t \xi^2 \mu} G(\alpha, \theta) t + \xi_0^2, \xi = x \text{ or } y \quad (1)$$

where

$$G(\alpha, \theta) = \frac{[\sin^2(\alpha - \theta) \tan(\alpha) - (\alpha - \theta) + \sin(\alpha - \theta) \cos(\alpha - \theta)]}{\tan(\alpha) \sin(\alpha - \theta)} \quad (2)$$

In equations (1) and (2), η refers to the filling factor, h_0 is the average height of the grooves formed by microstructures, τ is the tortuosity that is used to characterize the rough surface, σ is the surface tension, μ is the viscosity, α is the groove angle and θ is the contact angle. $G(\alpha, \theta)$ is a dimensionless factor associated with topographical features and properties of liquid metal. The derivation and details about equation (1) and (2) are illustrated in authors' recent study [9].

It is clearly indicated in figure 5 that the kinetics of imbibition on IMC2 during capillary viscous stage follows Washburn-type relation, equation (1). This confirms the kinetics model, equation (1) and (2).

DISCUSSION

It has been established that the early state of the imbibition of molten metal is driven by the capillary force and retarded by the viscous force [7-9]. The kinetics is described by balancing those two forces and a Washburn-type relation can be obtained as a result. For a radial imbibition configuration as indicated in figure 1, the central material source is of a finite mass and the imbibition will be slowed down by the exhaustion of the liquid source. The height of liquid metal contained in the roughness composed of microstructures will decrease over time thus reducing the capillary driving force.

Moreover, the kinetics is governed by the topographical features of the surface, which can be characterized with porosity/tortuosity [7-9]. It is clearly illustrated in figure 4 that the microstructures on the IMC2 and IMC3 cause the anisotropic imbibition. In [9] it is proved that the imbibition is preferential, associated with the direction of the microstructures. In this study, it is demonstrated that the IMC3 has a more pronounced orientation compared to the IMC2 so the imbibition on it indicates a larger extent of anisotropy in terms of a larger directional imbibition ratio. This offers a possible method to control or tune the flow of molten metal by an alteration of the surface topography, induced by grain growth.

CONCLUSION

The imbibition of a molten metal system on a rough inert intermetallic surface (IMC2) was in situ studied at an elevated temperature by using hot stage microscopy. The non-uniform spreading pattern was documented. The kinetics data indicate that the imbibing follows a Washburn-type relation ($\xi \sim t^{0.5}$) during the early stage and then deviates due to the impact of finite-size material source before the ultimate asymptotic termination. A theoretical model was verified, indicating a validity of the Washburn-type imbibition during the early capillary-viscous stage. This study further confirms the experimental evidence and justifies the theoretical framework proposed in previous studies for the imbibition on IMC1 and IMC3.

The results indicate that the final imbibition pattern can be tuned and controlled by the topographical features generated by the grain growth. So, this study offers (i) an experimental evidence that the molten metal flow can be tuned, and (ii) a

theoretical explanation for the molten metal imbibing on such substrates.

REFERENCES

- [1] de Gennes, P.G. Wetting: statics and dynamics, *Reviews of Modern Physics*, Vol. 57, No. 3, 1985, pp.827-863
- [2] Reyssat, M., Courbin, L., Reyssat, E., Stone, H.A. Imbibition in geometries with axial variations. *J. Fluid Mech.* Vol. 615, 2008, pp. 334-344
- [3] Warrick, A. W. *Soil Water Dynamics*. Oxford University Press: Oxford, 2003
- [4] Kuang-Han, C., Rong, X. and Evelyn, N. W. Uni-directional liquid spreading on asymmetric nanostructured surfaces, *Nature Materials*, Vol. 9, 2010, pp. 413-417
- [5] Chung, J. Y., Youngblood, J. P., Stafford, C. M. Anisotropic wetting on tunable micro-wrinkled surfaces. *Soft Matter*, Vol. 3, 2007, pp. 1163-1169
- [6] Gleiche, M., Chi, L. F. & Fuchs, H. Nanoscopic channel lattices with controlled anisotropic wetting, *Nature*, Vol. 403, 2000, pp. 173-175
- [7] Liu, W. and Sekulic, D. P. Capillary driven molten metal flow over topographically complex substrates. *Langmuir* 2011, 27, 6720-6730
- [8] Liu, W., Li, Y., Cai, Y., Sekulic, D. P. Capillary Rise of Liquids over a Microstructured Solid Surface. *Langmuir* 2011, 27, 14260-14266
- [9] Liu, W., Lu, L., Li, Y., Cai, Y., Sekulic, D. P. Preferential spreading of molten metal over an anisotropically microstructured surface. *EPL*. 2012, 97, 46003.
- [10] Zhao, H., Wang, H., Sekulic, D.P., Qian, Y. Spreading Kinetics of Liquid Solders over an intermetallic solid surface, Part 1: Lead-free solders, *Journal of Electronic Materials*, Vol.38, 2009, pp.1838-1845
- [11] Yost, F. G.; Rye, R. R.; Mann, J. A., Jr. Solder wetting kinetics in narrow v-grooves. *Acta Materilia*, 1997, 45, 5337-5345.